Low-temperature thermoelectric properties of $Yb_{14}MSb_{11}$ (M = Mn, Zn)

2007 J. Phys.: Condens. Matter 19 376211

(http://iopscience.iop.org/0953-8984/19/37/376211)

J. Phys.: Condens. Matter **19** (2007) 376211 (6pp) doi:10.1088/0953-8984/19/37/376211

Low-temperature thermoelectric properties of $Yb_{14}MSb_{11}$ (M = Mn, Zn)

R A Ribeiro[1], Y Hadano[2], S Narazu[2], K Suekuni[2], M A Avila[2] and T Takabatake[1,2]

[1] Institute for Advanced Materials Research, Hiroshima University, Higashi-Hiroshima 739-8530, Japan
[2] Department of Quantum Matter, ADSM, Hiroshima University, Higashi-Hiroshima 739-8530, Japan

Received 10 April 2007, in final form 25 July 2007
Published 22 August 2007
Online at stacks.iop.org/JPhysCM/19/376211

Abstract

We have synthesized $Yb_{14}MnSb_{11}$ and $Yb_{14}ZnSb_{11}$ to study the thermoelectric properties at low temperature ($4 < T < 300$ K). The materials were characterized by means of susceptibility (χ), resistivity (ρ), thermopower (S) and thermal conductivity (κ) measurements. The $\kappa(T)$ is dominated by phonon heat transport, and the Jahn–Teller effect in the $MnSb_4$ tetrahedra does not make a significant contribution to the reduction of the thermal conductivity at intermediate temperatures and above. A sharp minimum in $\kappa(T)$ for M = Mn occurs in the ferromagnetic transition at $T_C = 54$ K. The thermopower for $Yb_{14}MnSb_{11}$ is positive and increases upon heating, while that for $Yb_{14}ZnSb_{11}$ exhibits a negative peak at 60 K, before increasing and becoming positive. These different behaviors support the assertion that the Yb ions are in a divalent state in the former and in a valence fluctuating state in the latter.

1. Introduction

$Yb_{14}MnSb_{11}$ was recently reported by Brown *et al* [1] as a high-performance high-temperature thermoelectric material (400 K $< T <$ 1300 K). This Zintl compound was first synthesized by Chan *et al* [2] and belongs to the $A_{14}MPn_{11}$ family of compounds, with $I4_1/acd$ (No. 142) tetragonal structure [3]. The A cations are mostly in divalent states such as those of alkaline earth or rare earth atoms, with M = Mn, Al, Ga, In, Nb and Zn, and with Pn as a pnictogen atom. One formula unit is composed of 14 A^{2+} cations, one MPn_4^{9-} tetrahedron [$M^{3+}Pn_4^{3-}$], one Pn_3^{7-} polyatomic anion unit and four Pn^{3-} isolated anions [3–6].

This family shows complex atomic and magnetic structures which vary from paramagnetic insulators to ferromagnetic metals; for example: $Eu_{14}ZnSb_{11}$ shows a colossal magnetoresistance effect associated with a ferromagnetic transition coupled to a metal–insulator one [7]; $Ca_{14}MnSb_{11}$ and $Eu_{14}MnSb_{11}$ show an antiferromagnetic transition [8];

0953-8984/07/376211+06$30.00

$Yb_{14}MnSb_{11}$ presents a ferromagnetic transition at $T_C \sim 50$ K, and is a rare example of a d-electron heavy-fermion compound. The magnetic exchange interaction in this compound has been attributed to Rudermann–Kittel–Kasuya–Yosida (RKKY) interactions between localized moments on the Mn ions via conduction electrons. Also, the compounds of the 14–1–11 family display steric effects in the MSb_4 tetrahedron, and the $MnSb_4$, compared with the main group analogs, is most distorted due to the Jahn–Teller effect [9]. Optical conductivity measurements have shown that $Yb_{14}MnSb_{11}$ has a balance between carrier mediated ferromagnetism, and the Kondo and Jahn–Teller effects [10]. $Yb_{14}ZnSb_{11}$ was first synthesized by Fisher *et al* [11] and the observation of a maximum in the magnetic susceptibility at ∼85 K suggests an intermediate Yb valence state. The intermediate state has been corroborated by observation of both Yb^{3+} and Yb^{2+} contributions in the x-ray photoemission spectra [12]. In this work we focus on $Yb_{14}MnSb_{11}$ and $Yb_{14}ZnSb_{11}$, to study the thermoelectric properties at low temperatures ($T < 300$ K).

2. Experimental details

Single crystals of $Yb_{14}MnSb_{11}$ and $Yb_{14}ZnSb_{11}$ were grown from Sn flux, following a procedure similar to that described by Fisher *et al* [13]. The initial mixture was prepared directly from the elements (Yb: Ames Laboratory 99.99%, Mn: 99.99%, Zn: 99.999%, Sb: 99.9999%, Sn: 99.999%) in a carbon-coated, evacuated and sealed silica tube. The tube was heated to 1100 °C and slowly cooled over 100 h to 700 °C, where the molten flux was separated by decanting.

Polycrystalline $Yb_{14}ZnSb_{11}$ was synthesized in an Mo crucible with reagents Yb:Zn:Sb in the proportions 14:1:11, respectively. The crucible was heated to 660 °C for 3 h, and this was followed by heating to 900 °C for 24 h and cooling down to room temperature in 24 h. The sample was ground and a similar ramp was repeated for homogenization. After that, the sample was ground and a high-density pellet was prepared by a spark-plasma sintering (SPS) technique using Dr. SINTER LAB (Sumitomo Coal Mining). The SPS was performed at 600 °C for 30 min in a vacuum.

Samples of the three batches were pulverized in a glovebox for powder x-ray diffraction measurements, which showed that all samples were single phase. The $Yb_{14}MnSb_{11}$ presents lattice parameters $a = 16.62$ Å and $c = 21.97$ Å, which correspond to the expected values [2]. The $Yb_{14}ZnSb_{11}$ single crystal shows lattice parameters, $a = 16.55$ Å and $c = 21.81$ Å, similar to those reported by Fisher *et al* [11]. $Yb_{14}ZnSb_{11}$ polycrystal showed approximately the same value for the a parameter, $a = 16.52$ Å, but a slightly increased c parameter, $c = 22.01$ Å. The chemical composition was determined by electron-probe microanalysis (EPMA) using a wavelength dispersive JEOL JXA-8200 system. The EPMA for the single crystal with Mn confirmed the stoichiometric 14:1:11 proportion in the crystal and found the Sn inclusions to be at less than 0.07%. The single crystal with Zn presents an average composition of $Yb_{14}Zn_{0.73}Sb_{10.98}Sn_{1.47}$ if we normalize the Yb composition to 14. This incorporation of 5.4% Sn into the $Yb_{14}ZnSb_{11}$ structure could be the cause of the Zn deficiency, and account for the differences in lattice parameter between the single-crystal and polycrystal samples.

Since we wish to focus on the intrinsic properties of these materials, we chose to perform the measurements on the single crystal of $Yb_{14}MnSb_{11}$ and the polycrystal of $Yb_{14}ZnSb_{11}$. The samples are cut in a bar shape and for the single crystals the c-axis is along the length. The magnetization M was measured by a SQUID magnetometer (Quantum Design MPMS) from 2 to 350 K. The electrical resistivity was measured by a DC four-probe method. The thermopower was measured using a home-made set-up with a differential method. The thermal conductivity was measured by a steady heat flow method from 4.2 to 300 K.

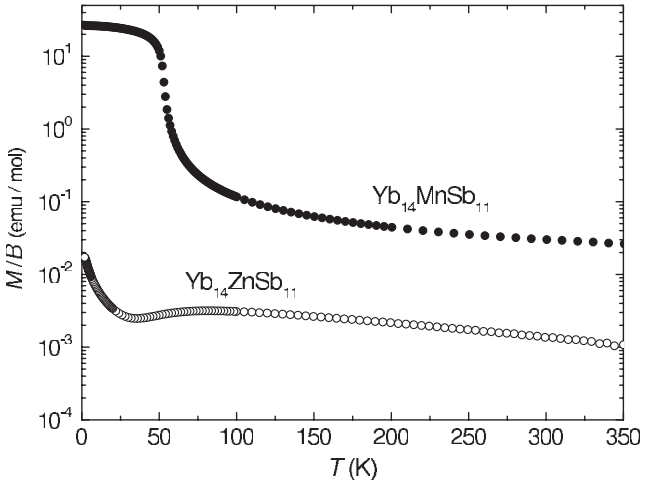

Figure 1. Temperature dependence of the magnetic susceptibility M/B at an applied field of 0.1 T for $Yb_{14}MnSb_{11}$ single crystal with $B \parallel c$ and $Yb_{14}ZnSb_{11}$ polycrystal.

3. Results and discussion

The temperature dependences of the magnetic susceptibility $\chi = M/B$ at an applied field of $B = 0.1$ T with $B \parallel c$ for the single crystals are shown in figure 1. A sharp ferromagnetic transition at $T_C \sim 54$ K is evident from the figure for the $Yb_{14}MnSb_{11}$ single crystal. The high-temperature behavior between 100 and 350 K can be fitted to a Curie–Weiss law if a constant offset, attributed to Van Vleck paramagnetism, is included: $\chi = C/(T-\theta) + \chi_0$. The fit results in an effective moment $\mu_{\text{eff}} = 4.16\ \mu_B$ f.u.$^{-1}$ and $\chi_0 = 3.62 \times 10^{-3}$ emu mol^{-1} for the $Yb_{14}MnSb_{11}$ single crystal. These values are consistent with previously published results [7, 13]. The $\chi(T)$ for $Yb_{14}ZnSb_{11}$ polycrystal presents a broad maximum at 85 K, as was reported previously [11]. Such behavior can be the manifestation of a valence fluctuating system. However, at temperatures above 150 K, it shows an effective moment of $\mu_{\text{eff}} = 1.88\ \mu_B$ f.u.$^{-1}$ or $\mu_{\text{eff}} = 0.13\ \mu_B$/Yb. Although this value is in good agreement with comparable data reported previously [11], such a small value of μ_{eff}, plus the tail at lowest temperatures, could be interpreted as indicating small amounts of free Yb^{3+} impurities. We will show below that the thermoelectric measurements give stronger evidence of intermediate Yb valence.

Figure 2 shows $\rho(T)$ for the single crystal and polycrystal of $Yb_{14}ZnSb_{11}$, and the single crystal of $Yb_{14}MnSb_{11}$. The behavior of $Yb_{14}MnSb_{11}$ is similar to that described by Fisher *et al* [11, 13]. The resistivity has a sharp drop below $T_C = 54$ K due to loss of spin-disorder scattering. Conversely, the $Yb_{14}ZnSb_{11}$ single crystal was measured along the c-axis and has a shoulder moved to lower temperature than that reported previously [11]. The $Yb_{14}ZnSb_{11}$ polycrystal presented a higher level of resistivity as expected from Matthiessen's rule, due to scattering by grain boundaries and disorder [14].

Among various transport properties, the thermopower S constitutes a simple and sensitive tool for detecting scattering mechanisms that dominate the electronic conduction and is less affected by the presence of grain boundaries, but so far this property has not been explored in $A_{14}MPn_{11}$ systems at low temperatures. The temperature variation below 300 K of $S(T)$ is displayed in figure 3. For the $Yb_{14}MnSb_{11}$ single crystal, $S(T)$ assumes positive values over

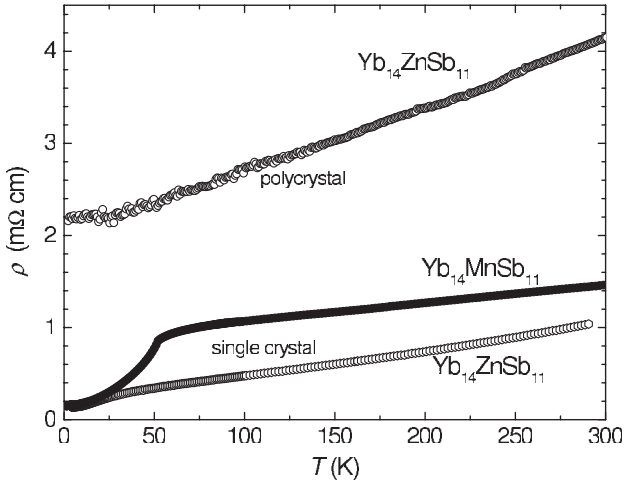

Figure 2. Temperature dependence of the electrical resistivity $\rho(T)$ of the polycrystal and single crystal of $Yb_{14}ZnSb_{11}$ and single crystal $Yb_{14}MnSb_{11}$. The single-crystal samples measurements were with $I \parallel c$.

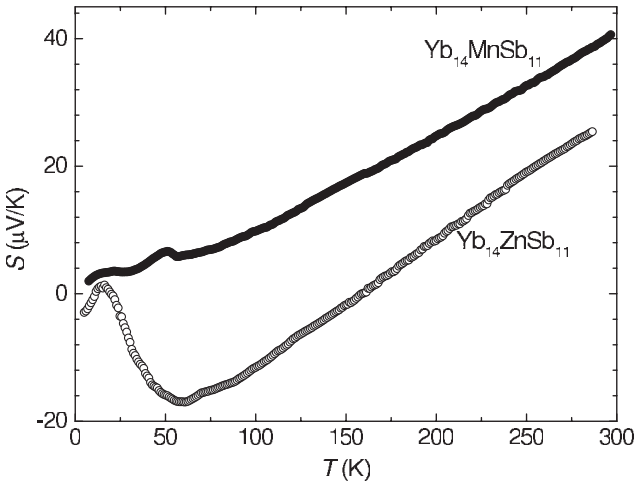

Figure 3. Temperature dependence of the thermopower $S(T)$ of $Yb_{14}MnSb_{11}$ single crystal along the c-axis (solid circles) and $Yb_{14}ZnSb_{11}$ polycrystal (open circles).

the whole measured temperature range. The $S(T)$ curve shows an upturn below T_C and goes through a local maximum with decreasing temperature.

Zlatic and Monnier published an extensive theoretical work on the thermopowers of Ce- and Yb-based compounds [15]. The ytterbium intermetallic compounds can be classified using their system in three types: (I) 'type a'— $S(T)$ has a negative minimum at high temperatures and a positive maximum at low temperatures due to a well defined local moment in Yb ions; (II) 'type b'— $S(T)$ has two minima separated by a small positive maximum; (III) 'type c'— $S(T)$ stays mostly negative, with a small local minimum, followed by a small local maximum, and a large, broad minimum in the range of 40–100 K.

For $Yb_{14}MnSb_{11}$ and $Yb_{14}ZnSb_{11}$, $S(T)$ is linear with temperature above 100 K, which is consistent with the linear dependence observed for 300–1000 K [1]. The low-temperature

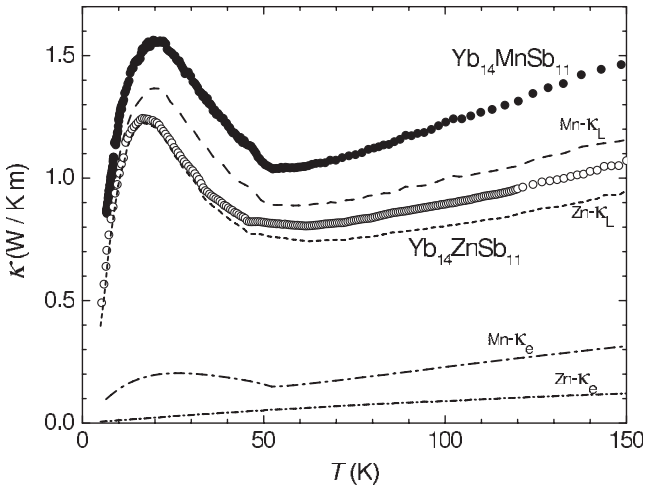

Figure 4. Temperature dependence of the thermal conductivity $\kappa(T)$ at low temperatures for $Yb_{14}MnSb_{11}$ single crystal along the c-axis (solid circles) and $Yb_{14}ZnSb_{11}$ polycrystal (open circles) at zero field. Mn(Zn)-κ_L and Mn(Zn)-κ_e correspond to the lattice and electronic components of $\kappa(T)$, respectively.

$S(T)$ for $Yb_{14}MnSb_{11}$ shows a minor perturbation at 50 K due to the Mn magnetic ordering, and $S(T)$ for $Yb_{14}ZnSb_{11}$ seems to be dominated by contributions from valence fluctuating Yb ions. If we subtract the T-linear background and consider only the Yb contribution, the behavior can be considered as that of a 'type c' Yb system, as per the above classification [15], with energy scale T^* in the range of 30–70 K [15, 16]. This behavior is similar to those of other Yb mixed valence systems such as $YbPdCu_4$ [17] and $YbNiSi_3$ [18].

The $\kappa(T)$ below 150 K for $Yb_{14}MnSb_{11}$ single crystal along the c-axis and $Yb_{14}ZnSb_{11}$ polycrystal samples are shown in figure 4. Generally, $\kappa(T)$ is given as the sum of the electronic component, κ_e, and lattice or phonon component, κ_L. The κ_e value can be estimated from the Wiedemann–Franz law, $\kappa_e = L_0 T/\rho$, where $L_0 = 2.45 \times 10^{-8}$ W Ω K^{-2}. Because κ_e is approximately one order of magnitude smaller than $\kappa(T)$ for both samples, the behavior of $\kappa(T)$ arises mostly from κ_L.

Both samples show very small values of a few W K^{-1} m^{-1}, which is expected since this family of compounds has a large unit cell, thus increasing the phonon scattering and minimizing the lattice thermal conductivity. We observe that the $\kappa(T)$ curves for both samples initially decrease monotonically upon cooling, until reaching a local minimum. For $Yb_{14}ZnSb_{11}$ it is broad and at $T \simeq 60$ K. The minimum for $Yb_{14}MnSb_{11}$ single crystal is quite sharp and occurs at $T_C \simeq 54$ K. Optical studies on $Yb_{14}MnSb_{11}$ suggest that the disappearance of the Jahn–Teller distortion occurs in conjunction with (and might be the driving force of) a change in Mn valence state and the appearance of magnetic order [10], which should naturally lead to increasing of both the electron and the phonon mean free paths, explaining the abrupt transition as compared with the Zn sample.

4. Conclusion

We have carried out magnetic, electrical, thermopower and thermal conductivity measurements on $Yb_{14}MnSb_{11}$ and $Yb_{14}ZnSb_{11}$ for temperatures below 300 K. Susceptibility and thermopower data for $Yb_{14}ZnSb_{11}$ give strong evidence of a Yb mixed valence state.

The thermopower for $Yb_{14}MnSb_{11}$ is positive and increases upon heating, while that for $Yb_{14}ZnSb_{11}$ exhibits a negative peak at 60 K. The different behaviors suggest that the Yb ions in the former are in a divalent state, and in the latter they are in a valence fluctuating state. The thermal conductivity level for both samples is at just a few $W\,K^{-1}\,m^{-1}$ due to increased phonon scattering by the large unit cell, and is governed mostly by the lattice contribution. The dynamic Jahn–Teller effect does not make a significant contribution to reducing the thermal conductivity.

Acknowledgments

We thank Y Shibata for the electron-probe microanalysis performed at N-BARD, Hiroshima University. This work was financially supported by the Grant in Aid for Scientific Research (A), No 18204032 from the Ministry of Education, Culture, Sports, Science and Technology, Japan.

References

[1] Brown S R, Kauzlarich S M, Gascoin F and Snyder G J 2006 *Chem. Mater.* **18** 1873
[2] Chan J Y, Olmstead M M and Kauzlarich S M 1998 *Chem. Mater.* **10** 3583
[3] Cordier G, Schafer H and Stelter M Z 1984 *Z. Anorg. Allg. Chem.* **519** 183
[4] Kuromoto T Y, Kauzlarich S M and Webb D J 1992 *Chem. Mater.* **4** 435
[5] Kauzlarich S M, Kuromoto T Y and Olmstead M M 1989 *J. Am. Chem. Soc.* **111** 8041
[6] Kauzlarich S M 1990 *Comments Inorg. Chem.* **10** 75
[7] Chan J Y, Kauzlarich S M, Klavins P, Shelton R N and Webb D J 1997 *Chem. Mater.* **9** 3132
[8] Sanchez-Portal D, Martin R M, Kauzlarich S M and Pickett W E 2002 *Phys. Rev.* B **65** 144414
[9] Rehr A, Kuromoto T Y, Kauzlarich S M, Del Castillo J and Webb D J 1994 *Chem. Mater.* **6** 93
[10] Burch K S, Schafgans A, Sayles T A, Maple M B, Sales B C, Mandrus D and Basov D N 2005 *Phys. Rev. Lett.* **95** 046401
[11] Fisher I R, Bud'ko S L, Song C and Canfield P C 2000 *Phys. Rev. Lett.* **85** 1120
[12] Holm A P, Ozawa T C, Kauzlarich S M, Morton S A, Dan Waddill G and Tobin J G 2005 *J. Solid State Chem.* **178** 262
[13] Fisher I R, Wiener T A, Bud'ko S L, Canfield P C, Chan J Y and Kauzlarich S M 1999 *Phys. Rev.* B **59** 13829
[14] Kittel C 1976 *Introduction to Solid State Physics* 5th edn (New York: Wiley) p 171
[15] Zlatic V and Monnier R 2005 *Phys. Rev.* B **71** 165109
[16] Alami-Yadri K, Jaccard D and Andreica D 1999 *J. Low Temp. Phys.* **114** 135
[17] Casanova R, Jaccard D, Marcenat C, Hamdaoui N and Besnus M J 1990 *J. Magn. Magn. Mater.* **90** 587
[18] Avila M A, Sera M and Takabatake T 2004 *Phys. Rev.* B **70** 100409